A New Robotic 3D Inspection System of Automotive Screw Hole

Moon-Hong Baeg, Seung-Ho Baeg, Chanwoo Moon*, Gu-Min Jeong, Hyun-Sik Ahn, and Do-Hyun Kim

Abstract: This paper presents a new non-contact 3D robotic inspection system to measure the precise positions of screw and punch holes on a car body frame. The newly developed sensor consists of a CCD camera, two laser line generators and LED light. This lightweight sensor can be mounted on an industrial robot hand. An inspection algorithm and system that work with this sensor is presented. In performance evaluation tests, the measurement accuracy of this inspection system was about 200 μm, which is a sufficient accuracy in the automotive industry.

Keywords: 3D sensor, frame inspection, laser, screw hole, robotic 3D inspection system, vision.

1. INTRODUCTION

Productivity and quality of the finished car are important in automotive industry. To improve them, a high precision automatic system which inspects the quality of welds and assembly, alignment of holes and body fit is indispensable, and various inspection systems which use computer vision and laser sensor devices have been proposed [1-4]. Especially, the alignments of holes and parts are important, because imprecise positioning of punches and screw holes on a body frame can twist the frame, loosen screws, produce vibration and deteriorate other qualities. Therefore, these holes and parts need to be inspected with precision for high quality control. Perceptron, Inc. of USA released a non-contact 3D visual inspection system for the automotive industry [5], and two kinds of inspection methods were proposed. The first method uses multiple sensors which are arranged all over the body frame to measure the shape of the frame, but if the inspection points are changed, all sensors need to be rearranged. In the second method, the sensor system is mounted on a robot hand, and the robot inspects the target points whose positions are stored in advance.

Manuscript received June 5, 2007; revised January 14, 2008; accepted March 20, 2008. Recommended by Editorial Board member Sangdeok Park under the direction of Editor Jae-Bok Song.

Moon-Hong Baeg and Seung-Ho Baeg are with the Applied Robot Technology Division, KITECH, 1271-18 Sa 1-dong, Sangnok-gu, Ansan-si, Gyeonggi-do, Korea (e-mails: {mhbaeg, shbaeg}@kitech.re.kr).

Chanwoo Moon, Gu-Min Jeong, Hyun-Sik Ahn, and Do-Hyun Kim are with the College of Electrical Engineering & Computer Science, Kookmin University, 861-1, Jeongneung-dong, Seongbuk-gu, Seoul, Korea (e-mails: {mcwnt, gm1004, ahs, dhkim@kookmin. ac.kr).

* Corresponding author.

The latter method is preferred because of the flexibility of a robotic system, but this system has some inconveniences. Firstly, the gathered position data are expressed with respect to the sensor coordinate system, not to the reference coordinate system, and the inspection system only compares the obtained data with the model. Therefore, the body frame must be fixed at the exact position to inspect the actual position. Secondly, if the inspection point is not perpendicular to the sensor system, measurements become inaccurate. 3D laser scanners which inspect the surface of the object were commercialized by some vendors, but they have insufficient accuracy and require long measurement time to measure the precise position of a hole on-line. Vision systems which measure the positions of holes were reported [6,7], but they were inaccurate for the automotive industry. As a result, a new system to inspect the screws and punch holes of a frame was needed. This paper presents a new non-contact 3D robotic inspection system and an algorithm to measure the precise positions of screws and punch holes on an automotive body frame. A newly developed lightweight sensor, which consists of a CCD camera, two laser line generators and LED light can be mounted on the robot's hand to move from an inspection point to another inspection point as the robot is taught.

2. PROPOSED SENSOR SYSTEM

Not a few assembly operations are insertion operations of automotive parts into holes, and these holes are positioned all over the body frame. The holes located on the underbody of the frame can not be inspected with the established methods such as stereo vision and the laser light cut method [8,9].

To measure the precise 3D positions of these holes, a new sensor system which consists of a CCD camera, 2 laser line generators and LED light is proposed. A

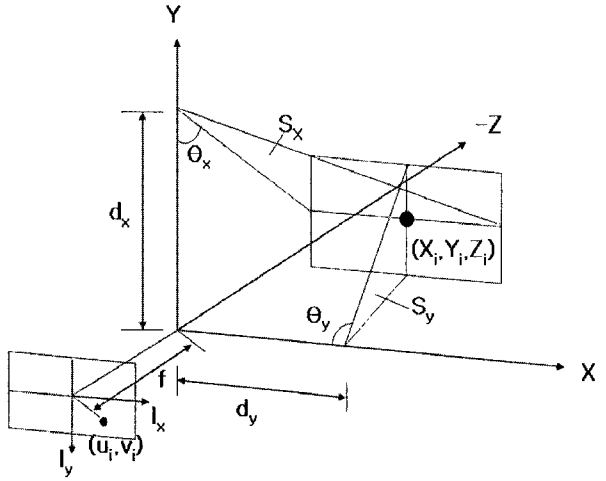

Fig. 1. Modeling of the proposed sensor system.

coordinate model of the proposed sensor system is depicted in Fig 1. The sensor coordinate is located in the center of the camera which is modeled as a pinhole camera, and two laser line generators, the X-laser and Y-laser, are located on the Y and X axis, respectively. A hole for inspection is on plane p.

Here,

d_x: Distance between X-laser and the camera coordinate

θ_x: Angle between X-laser and the camera coordinate

d_y: Distance between Y-laser and the camera coordinate

θ_y: Angle between Y-laser and the camera coordinate

f : Effective Focal Length

S_x: Slit beam of X-laser

S_y: Slit beam of Y-laser.

A point $P_i({}^C X_i, {}^C Y_i, {}^C Z_i)$ on the object which is spotted by laser beams S_x and S_y are projected onto (u_i, v_i) of the camera image, and by triangulation, the 3D position of this point is obtained as follows[10]. Firstly, the camera image (u_i, v_i) of this point is obtained as (1) and (2).

$$u_i = -\frac{f\,{}^c X_i}{{}^c Z_i} \tag{1}$$

$$v_i = -\frac{f\,{}^c Y_i}{{}^c Z_i} \tag{2}$$

Now, the plane equation of S_x is give as

$$\sin\theta_x({}^c Y - d_x) + \cos\theta_x\,{}^c Z = 0. \tag{3}$$

From (1)-(3), the 3D position of P_i is obtained as

$$\begin{aligned} {}^c X_i &= -\frac{u_i d_x \tan\theta_x}{f + v_i \tan\theta_x}, \\ {}^c Y_i &= -\frac{v_i d_x \tan\theta_x}{f + v_i \tan\theta_x}, \\ {}^c Z_i &= -\frac{f d_x \tan\theta_x}{f + v_i \tan\theta_x}. \end{aligned} \tag{4}$$

Using the Y-laser and by the same procedure, we find the position of P_i by

$$\begin{aligned} {}^c X_i' &= -\frac{u_i d_y \tan\theta_y}{f + u_i \tan\theta_y}, \\ {}^c Y_i' &= -\frac{v_i d_y \tan\theta_y}{f + u_i \tan\theta_y}, \\ {}^c Z_i' &= -\frac{f d_y \tan\theta_y}{f + v_i \tan\theta_y}. \end{aligned} \tag{5}$$

Procedure to calculate the 3D position of a hole is as follows.

Step 1: From the laser line image, calculate the plane equation of the surface which includes the hole

Step 2: From the camera image and result of Step 1, calculate the 3D positions of the boundary points of the hole

Step 3: With the result of Step 2, calculate the center position of the hole

This procedure can be described more in detail.

Step 1: Laser lines of X-laser and Y-laser are captured by the camera, as shown in Fig. 2. The 3D positions of the points on the laser lines can be found by (4) and (5).

The plane equation which contains m such points can be obtained by the least squares fitting by

$$\hat{A}X + \hat{B}Y + \hat{C}Z = -1, \tag{6}$$

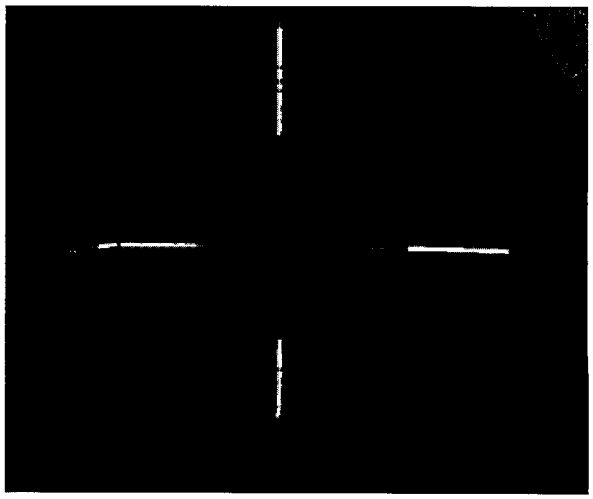

Fig. 2. Laser line image.

where

$$\hat{\theta}_m = \left(\sum_{i=1}^{m} \varphi_i \varphi_i^T\right)^{-1} \sum_{i=1}^{m} \varphi_i,$$
$$\hat{\theta}_m = \begin{bmatrix} \hat{A} \\ \hat{B} \\ \hat{C} \end{bmatrix}, \quad \varphi_i = \begin{bmatrix} X_i \\ Y_i \\ Z_i \end{bmatrix}. \tag{7}$$

Step 2: From the camera image of the object with LED lighting as shown in Fig. 3, and after processing it, we get the boundary points of the hole (u_i, v_i). Since this point lies on the plane of (6), we obtain (8) and (9).

$$\hat{A}\left(\frac{Z_i}{f}\right)u_i + \hat{B}\left(\frac{Z_i}{f}\right)v_i + \hat{C}Z_i = -1 \tag{8}$$

$$Z_i = \frac{f}{\hat{A}u_i + \hat{B}v_i + \hat{C}f}$$

$$X_i = \frac{Z_i}{f}u_i \tag{9}$$

$$Y_i = \frac{Z_i}{f}v_i$$

Step 3: By projecting the boundary points of Step 2 onto the X-Y plane, we obtain an ellipse as given by

$$\hat{a}X^2 + \hat{b}XY + \hat{c}Y^2 + \hat{d}X + \hat{e}Y + 1 = 0. \tag{10}$$

By least squares fitting, each parameter can be calculated by

$$\hat{\theta}_e = \left(\sum_{i=1}^{m} \varphi_i \varphi_i^T\right)^{-1} \sum_{i=1}^{m} \varphi_i,$$
$$\hat{\theta}_e = \begin{bmatrix} \hat{a} \\ \hat{b} \\ \hat{c} \\ \hat{d} \\ \hat{e} \end{bmatrix}, \quad \varphi_i = \begin{bmatrix} X_i^2 \\ X_i Y_i \\ Y_i^2 \\ X_i \\ Y_i \end{bmatrix}. \tag{11}$$

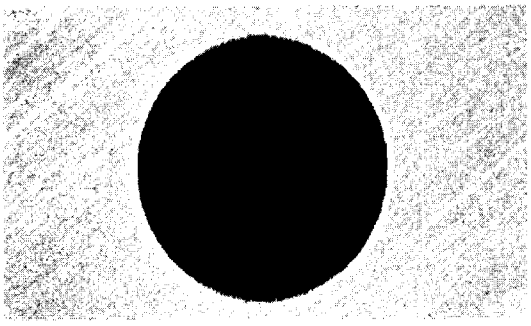

Fig. 3. Camera Image of hole with LED lighting.

Because this ellipse is a projection of a circle which is rotated and translated, to calculate the center of this ellipse, the ellipse needs to be rotated by

$$X = X'\cos\theta - Y'\sin\theta,$$
$$Y = X'\sin\theta + Y'\cos\theta. \tag{12}$$

By (11), (12) and by setting the coefficient of the product term of $X'Y'$ to 0, relation (13) is obtained.

$$\tan 2\theta = \frac{\hat{b}}{\hat{a} - \hat{c}} \tag{13}$$

After obtaining θ, and from (11) and (12), the coordinate transformed circle is obtained by (14) and (15).

$$a'X'^2 + c'Y'^2 + d'X' + e'Y' + 1 = 0 \tag{14}$$

$$a'(X' + \frac{d'}{2a'})^2 + c'(Y' + \frac{e'}{2c'})^2 = \frac{d'^2}{4a'} + \frac{e'^2}{4c'} - 1 \tag{15}$$

From (8) and (15), its center is obtained as in

$$(-\frac{d'}{2a'}, -\frac{e'}{2c'}, \frac{\hat{A}}{\hat{C}}\frac{d'}{2a'} + \frac{\hat{B}}{\hat{C}}\frac{e'}{2c'} - \frac{1}{\hat{C}}). \tag{16}$$

3. DEVELOPMENT OF THE PROPOSED SENSOR SYSTEM

A sensor system must have sufficient measurement accuracy, and it need to be sufficiently light in weight to be mounted on a commercial industrial robot. And to inspect the underbody of car frame, it needs to be small. Fig. 4 shows the developed sensor system. Two types of sensors are designed according to working distance which is the distance between the camera and object. The designed working distances are 100 mm and 150 mm. Table 1 provides the components list of this sensor system.

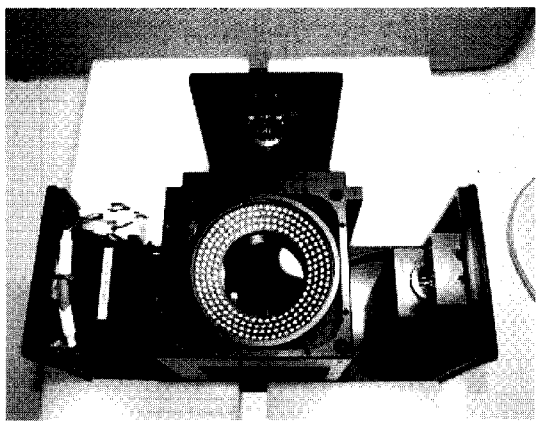

Fig. 4. The developed sensor with 100mm working distance.

Table 1. The component list of the developed sensor.

Part	Model	Specification
Area Scan CCD Camera	BASLER A101	1,300 (H) x 1,030 (V) pixels 2/3 inch HAD interline transfer progressive scan CCD
Lens	Working distance 100mm	
	Xenoplan F1.9/35 Lens	Effective Focal Length 34.9 mm Maximum distortion 0.25%
	Working distance 150mm	
	Apo-Componon F2.4/40 Lens	Effective Focal Length 41.5 mm Maximum distortion 0.5%
Laser Line Generator	13LR	Working distance 100mm
		Wave length 661nm Fan angle 25° Line length 74.7 mm Focus Range 100 ~ 205mm
		Working distance 150mm
		Wave length 661nm Fan angle 12° Line length55.9 mm Focus Range 205 ~ 415mm
Lightning LED	LDR-90B LED	LED Color RED Power Consumption 9.5W

4. EXPERIMENT

Fig. 5. shows a general view of the proposed inspection system. A developed sensor is mounted on a robot's hand, and the entire inspection process is controlled by a process control PLC (Programmable Logic Controller). The measurement data are gathered by PC. Fig. 6 shows an experimental setup for the evaluation of the inspection performance. The performance is evaluated with a gauge block which has test holes, as shown in Fig. 7. The gauge block is made of Al, tested previously with a commercial 3D coordinate measurement machine, and it has machining error of less than ±5μm. Fig. 8 shows a captured inspection image.

To evaluate the repeatability measurement accuracy of the sensor only, the robot arm is fixed over a target hole of the gauge block, and the sensor measures the position of the target hole repetitively. In the first experiment, the target hole is perpendicular to the sensor, and obtained repeatability measurement accuracy is nearly 0. In the second experiment, the target hole is not perpendicular with arbitrary angles, and repeatability measurement accuracy is about 23 μm, which is less than the error of 1 pixel, 40 μm.

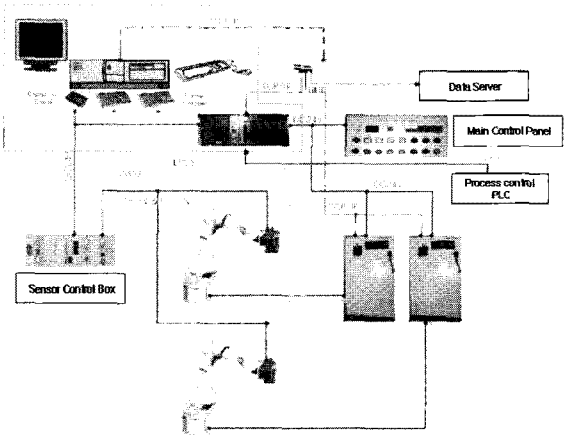

Fig. 5. Construction of proposed inspection system.

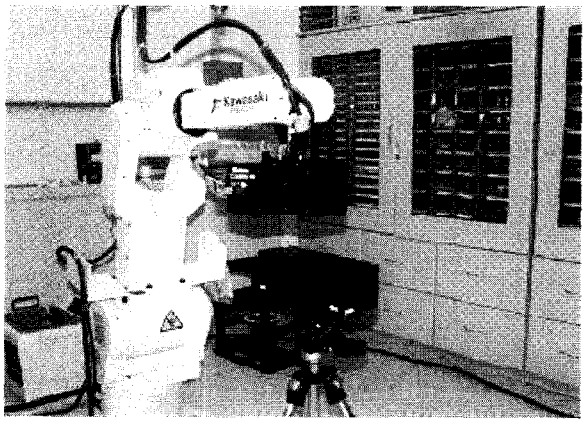

Fig. 6. Experimental Setup.

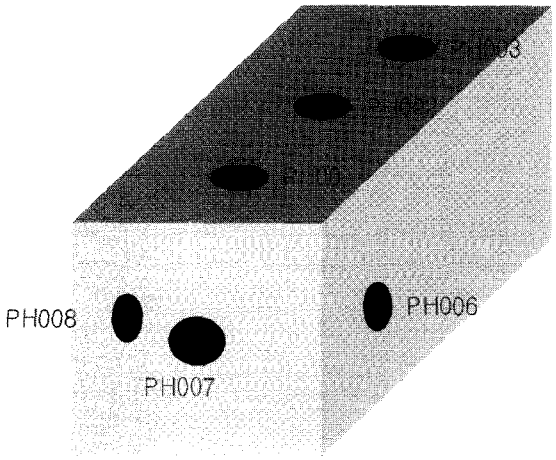

Fig. 7. CAD drawing of gauge block for the performance evaluation.

Table 2 summarizes the experimental results. The measurement accuracy of the whole inspection system is evaluated in a similar way. Firstly, the robot hand moves over the target hole, the sensor measures the position of the hole, and then the acquired data are transformed to the base coordinate system from the sensor coordinate system. Table 3 shows the results of the repetitive experiment, and shows that the

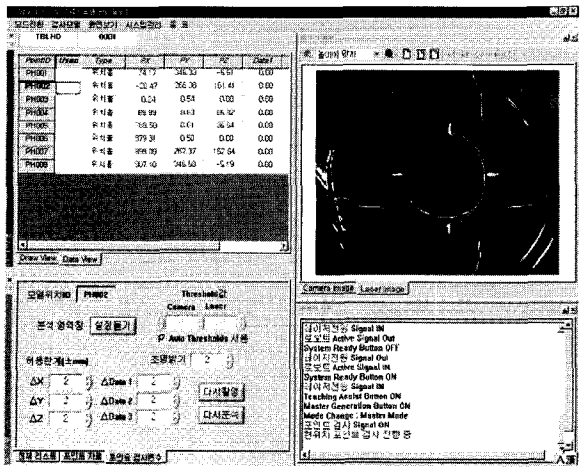

Fig. 8. Captured inspection image.

Table 2. Repeatability measurement accuracy of the proposed sensor.

Itera -tion	Experiment 1 (mm) (Perpendicular)				Experiment 2 (mm) (Out of perpendicular)			
	SSR PX	SSR PY	SSR PZ	SSR D1	SSR PX	SSR PY	SSR PZ	SSR D1
1	0.002	-0.017	-245.520	10.108	-0.143	-0.665	-245.518	8.612
2	0.001	-0.013	-245.520	10.108	-0.143	-0.667	-245.520	8.612
3	0.002	-0.019	-245.521	10.108	-0.144	-0.669	-245.518	8.612
4	0.001	-0.018	-245.519	10.148	-0.142	-0.644	-245.519	8.612
5	0.002	-0.019	-245.519	10.108	-0.143	-0.670	-245.518	8.612
6	0.001	-0.015	-245.519	10.108	-0.141	-0.598	-245.519	8.612
7	0.003	-0.017	-245.520	10.108	-0.143	-0.668	-245.519	8.612
8	0.003	-0.017	-245.520	10.148	-0.143	-0.668	-245.519	8.612
9	0.001	-0.017	-245.520	10.108	-0.142	-0.644	-245.520	8.612
10	0.001	-0.017	-245.518	10.148	-0.143	-0.671	-245.517	8.612
Max	0.003	-0.013	-245.518	10.148	-0.141	-0.598	-245.517	8.612
Min	0.001	-0.019	-245.521	10.108	-0.144	-0.671	-245.520	8.612
Range	0.002	0.005	0.003	0.040	0.003	0.073	0.003	0.000
σ	0.001	0.002	0.001	0.019	0.001	0.023	0.001	0.000

maximum deviation is less than 40 μm. Table 4 summarizes the performance of this sensor system.

5. CONCLUSION

To improve the productivity and quality of automotive parts, a high precision inspection system is essential. In this paper, a new sensor system was developed, and an on-line high speed and high accuracy 3D inspection system equipped with this sensor system was presented. This inspection system can inspect the 3D positions of punching holes and screw holes, which are scattered all over the car body

Table 3. Repeatability measurement accuracy of the proposed inspection system.

Iteration	PX (mm)	PY (mm)	PZ (mm)
1	29.313	920.674	343.787
2	29.317	920.669	343.787
3	29.309	920.663	343.787
4	29.309	920.665	343.789
5	29.310	920.671	343.796
6	29.312	920.669	343.786
7	29.309	920.668	343.780
8	29.336	920.665	343.782
9	29.332	920.665	343.785
10	29.338	920.666	343.779
Maximum	29.338	920.674	343.796
Minimum	29.309	920.663	343.779
Range	0.029	0.011	0.017
σ	0.012	0.003	0.005

Table 4. Specification of the proposed inspection system.

Features	Unit	Specification
Inspection system measurement accuracy	μm	± 215
Measurement accuracy of sensor	μm	23
Inspection system repeatability measurement accuracy	μm	±40
Working Distance	mm	100, 150
Measurement time	Second/Point	3.5
Weight of sensor	kg	5.7

frame. The newly developed sensor, which consists of a CCD camera, 2 laser line generators and LED lightning, was mounted on an industrial robot, and inspection points were programmed previously by teaching. The inspection system adopting this sensor system is controlled by a process control PLC, and the measurement data are gathered and analyzed by PC. Experiments to measure the accuracy of this sensor system were conducted with a precisely manufactured gauge block. The accuracy of the developed sensor was 23 μm, and in the experiment using the sensor installed on a robot, the accuracy of the inspection system was 215 μm. This deterioration is due to the inaccuracy of the robot. Measurement accuracy of ±0.2 ~ 0.25mm must be guaranteed in the automobile industry, and these results show that our sensor system is acceptable. Now, these sensors are under testing in

three automotive factories, and as a future work, a research on the calibration of the robot will be studied to improve the measurement accuracy of the sensor system.

REFERENCES

[1] P. Marino, M. Dominguez, and M. Alonso, "Inspection of steel sheets based on CCD image sensors," *Proc. of IEEE/SICE/RSJ International Conference on Multisensor Fusion and Integration for Intelligent Systems*, pp. 68-73, August 1999.

[2] M. Kondo, S. Tachiki, M. Ishida, and K. Higuchi, "Automatic measuring system for body fit on the automobile assembly line," *Proc. of IEEE International Conference on Robotics and Automation*, pp. 538-543, 1995.

[3] Q. Shi, N. Xi, H. Chen, and Y. Chen "Calibration of robotic area sensing system for dimensional measurement of automotive part surfaces," *Proc. of IEEE/RSJ International Conference on Intelligent Robots and Systems*, pp. 1526-1531, August 2005.

[4] F. Shafait, M. S. Pervez, A. A. Qazi, J. Wollnack, and T. Trittin "Real time two-step inspection system for assembled valve keys in automobile cylinder heads," *Proc. of third International Conference on Image and Graphics*, pp. 520-523, December 2004.

[5] *Scanworks Datasheet*, Perceptron, 2005.

[6] B. Lara, K. Althoefer, and L. D. Seneviratne "Automated robot-based screw insertion system," *Proc. of the 24th Annual Conference of the IEEE, Industrial Electronics Society,* Volume 4, pp. 2440-2445, Aug. 31 - Sept. 4 1998.

[7] W. J. Pastorius, "MACHINE vision for industrial inspection metrology and guidance," *Proc. of Programmable Control and Automation Technology Conference and Exhibition*, pp. 13A2 - 1/1-5, Oct. 12-13 1988.

[8] R. Jain, R. Kasturi, and B. G. Schunck, *Machine Vision*, 1st edition, McGraw-Hill Science/Engineering/ Math, March 1, 1995.

[9] F. Chen, G. M. Brown, and M. Song, "Overview of three-dimensional shape measurement using optical methods," *Optical Engineering*, vol. 39, no. 1, pp. 10-22, 2000.

[10] R. A. Jarvis, "A perspective on range-finding techniques for computer vision," *IEEE Trans. on Pattern Analysis Machine Intelligence*, vol. 5, no. 2, pp. 122-139, 1983.

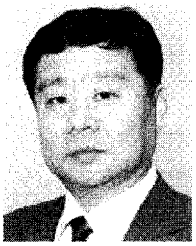

Moon-Hong Baeg received the B.S. and M.S degrees in Control Engineering from Seoul National University, and the Ph.D degree from University of Tokyo in 1982, 1984 and 1995, respectively. His research inter-ests include robotics vision inspection, 3-D scene analysis and robot naviga-tions.

Seung-Ho Baeg received the B.S. and M.S degrees in Metallurgical Engineering from Korea University in 1991 and 1993, respectively. His research interests include machine vision inspection, 3D image acquisi-tion and mobile robot navigations.

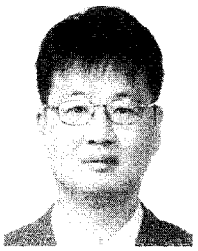

Chanwoo Moon received the Ph.D. degree in Electrical Engineering and Computer Science from Seoul National University in 2001. His research interests include mobile robot navigation/localization, micro manipulation and motor control.

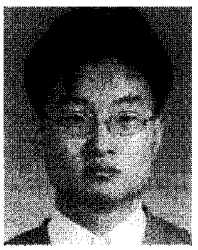

Gu-Min Jeong received the Ph.D. degree in Electrical Engineering and Computer Science from Seoul National University in 2001. His research interests include embedded system, PDA application and vehicle electronics.

Hyun-Sik Ahn received the Ph.D. degree in Control and Instrumentation from Seoul National University in 1992. His research interests include embedded system, vehicle electronics and control.

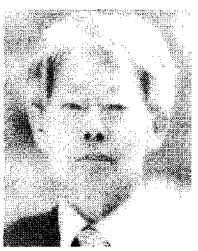

Do-Hyun Kim received the Ph.D. degree in Electronics Engineering from Seoul National University. He was a President of IEEK in 2000. His interests include control and instrumentation.